8th International Symposium on Magnetic Bearing
August 26-28, 2002, Mito, Japan

POSITION SELF-SENSING CONTROL OF AN AXIAL SELF-BEARING MOTOR

Satoshi Ueno
Dept. of Intelligent Machines and System Eng., Faculty of Science and Technology,
Hirosaki University, 3 Bunkyo-cho, Hirosaki, Aomori, 036-8561, Japan
ueno@cc.hirosaki-u.ac.jp

Ken-ichi Matsuda
Dept. of Mechanical Eng., Ibaraki University, Hitachi, Ibaraki-Pref., 316-8511 Japan,
matsu@mech.ibaraki.ac.jp

Hiroshi Sato
Dept. of Intelligent Machines and System Eng., Faculty of Science and Technology,
Hirosaki University, 3 Bunkyo-cho, Hirosaki, Aomori, 036-8561, Japan
satoh@cc.hirosaki-u.ac.jp

Yohji Okada
Dept. of Mechanical Eng., Ibaraki University, Hitachi, Ibaraki-Pref., 316-8511 Japan,
okada@mech.ibaraki.ac.jp

ABSTRACT

This paper introduces a position self-sensing technique for an axial self-bearing motor where the flat disc alternating current (AC) motor has both rotation and axial position control capability. The axial self-bearing motor has simpler construction than that of the radial self-bearing motor. In addition, the design of the control system can be simplified since the hardware components can be reduced. However, a displacement sensor is required to control the axial position, and it is obstacle of cost reductions, miniaturization and flexible system design. To solve this problem, position self-sensing technique is applied to the axial self-bearing motor. When a pulse width modulated switching amplifier drives the stator windings, the current waveform has a high frequency ripple which includes an air gap information. By demodulating this ripple, the displacement of the rotor can be estimated. In this paper, theoretical analysis, numerical simulation and experiments are carried out to examine fundamental self-sensing property.

INTRODUCTION

Recently, active magnetic bearings have been used widely due to their noncontact supporting capability. For many applications, a rotary motor is installed between the radial magnetic bearings significantly increasing both machine size and weight. The structure of magnetic bearings is very similar to that of an AC motor, hence a self-bearing motor (bearing less motor, combined motor-bearing) has been developed and reported. The self-bearing motor can be classified into two types, according to the controlled axis; one is the radial type and the other is the axial type. The radial self-bearing motor can be control two degrees of the radial motion of the rotor [1, 2, 3]. However it has complex stator construction and control system because it requires two components of rotating magnetic flux. On the other hand, the axial self-bearing motor controls only axial motion actively, and it has simpler construction and control system than that of the radial self-bearing motor [4, 5]. However, a displacement sensor is required to control the axial position, and it is obstacle of cost reductions, miniaturization and flexible system design. To solve this problem, a position self-sensing technique is applied to the axial self-bearing motor.

A position self-sensing technique for the active magnetic bearing and the radial self-bearing motor has been investigated by many researchers. The self-sensing technique can be classified into two methods; the observer type [6] and the modulation type [7, 8, 9, 10]. The former method is realized at low cost, but it has drawbacks of poor robustness and poor disturbance rejection. The later one requires the additional hardware, but it can improve the drawbacks

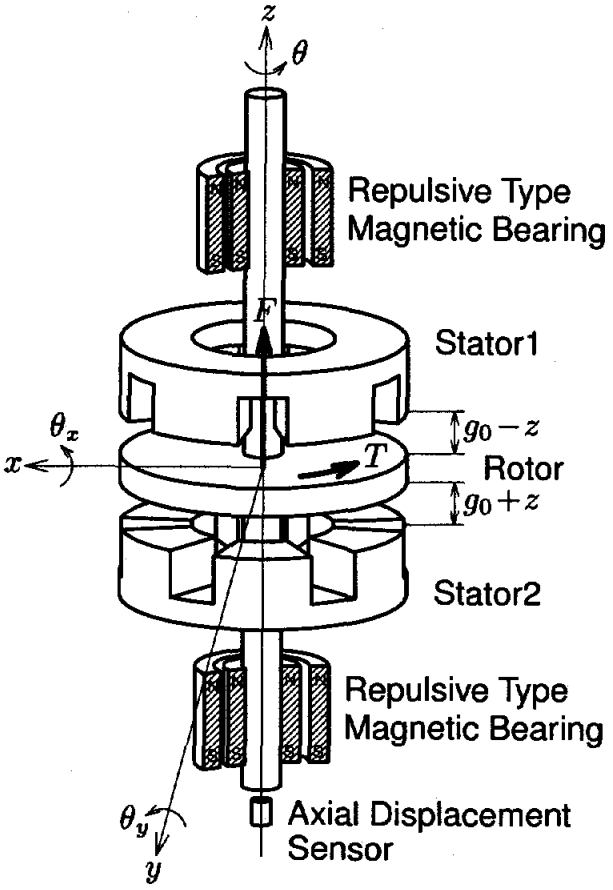

FIGURE 1: Axial Self-Bearing Motor

of the former methods. In this paper, a method proposed by Okada et al. [8] is utilized for the axial self-bearing motor. This method estimates the air gap length by demodulating the switching frequency component of the current waveform driven by the PWM amplifier. Since the air gap length modulates the amplitude of the switching waveform, the switching frequency component of the current is the direct indication of displacement. With this method, special amplifier or additional winding are not required, self-sensing can be realized relatively easily.

In this paper, the self-sensing output of the axial self-bearing motor is analyzed theoretically, and the proposed method is confirmed both in simulation and experiment. Then the possibility of the self-sensing control of the axial self-bearing motor is discussed.

AXIAL SELF-BEARING MOTOR

The axial self-bearing motor consists of a disc rotor with the stator on one side (unidirectional type) or on both side (bi-directional type) of the rotor. Figure 1 shows the schematic of a bi-directional axial self-bearing motor. The axial motion of the rotor is actively controlled while the other axes are constrained by additional passive or active magnetic bearings. The axial self-bearing motor provides the motoring torque around the z axis, and controls the position of the rotor along this axis.

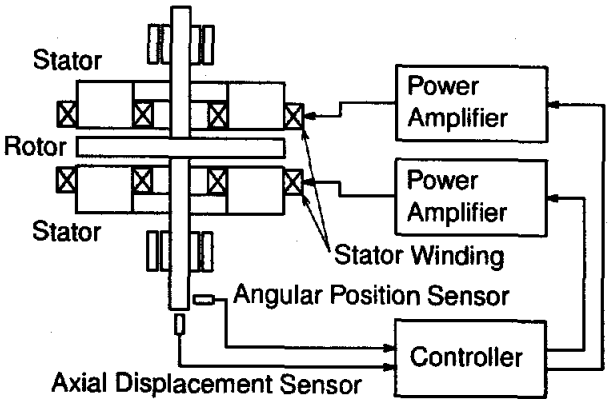

FIGURE 2: Control System of Axial Self-Bearing Motor

The stator produces a rotating magnetic flux in the air gap, to generate the motor torque. The axial force is controlled by changing the amplitude of the rotating flux. Since a single rotating magnetic flux is capable of generating both the motoring torque and the axial force, the axial self-bearing motor has simpler construction than that of the radial self-bearing motor. In addition, the design of the control system can be simplified since the hardware components can be reduced. Figure 2 shows the schematic of the control system of the axial self-bearing motor using the repulsive type radial magnetic bearings.

The axial self-bearing motor can be realized as permanent magnet, induction, and reluctance motor. However, only the permanent magnet motor is tested in this paper, because it is the most efficient, and has the possibility for many applications.

POSITION SELF-SENSING

Generally, 3-phase windings and 3-phase PWM inverters are employed for an AC motor. However, it is difficult to obtain the estimated air gap length independently of the angular position of the voltage vector driven by the 3-phase PWM inverter, because the voltage and current of each winding affects each other. In order to avoid this problem, 2-phase windings as shown in figure 3 are employed for stator windings and each pole is driven by two single phase PWM amplifier. Since each winding is placed at 90 degrees apart in the 2-phase winding, mutual-inductance becomes zero. Hence there is no interference between them, and it is considered that the self-sensing can be realized easily.

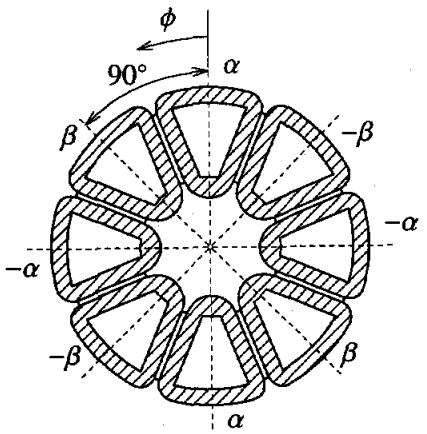

FIGURE 3: 2-phase Windings

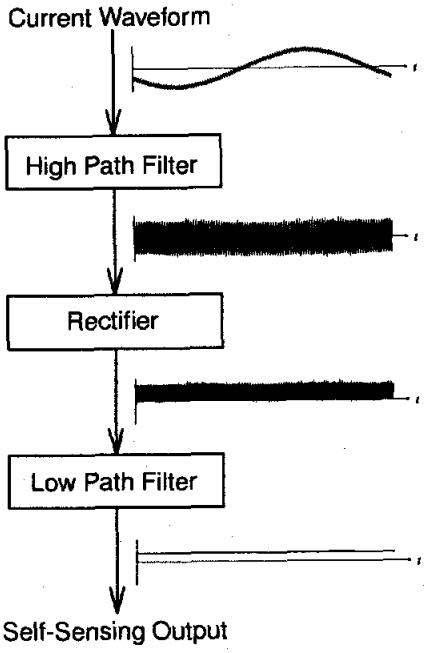

FIGURE 4: Self-Sensing Filter

General Approach

A filter shown in figure 4 that consists of high pass filter, rectifier, and low pass filter is used to obtain the amplitude of the switching frequency component of the current waveform. The current waveform is applied to a high pass filter at first. This filter should block all frequencies lower than the lowest frequency components in the expected switching waveform. The amplitude of the resulting waveform is measured by rectifying the signal and then averaging over some time scale, ideally a multiple of the switching waveform period. Such averaging is carried out by an ideal low pass filter which blocks all frequencies higher than the inverse of the selected time scale.

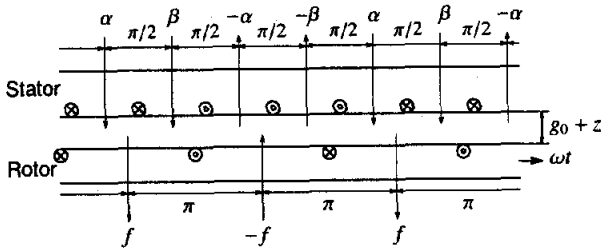

FIGURE 5: Coordinate System

Analytical Consideration

The coordinate axis of the magnetic paths are defined as shown in figure 5. This figure shows the axial motor unwrapped along its circumference and the angle is the electric angle. The stator has 2-phase winding denoted α and β placed at $\pi/2$ and the rotor has a single winding f. Here, the rotor's permanent magnet have been replaced by an equivalent rotor current i_f. The α and β axes show the direction of the flux produced by each winding.

The self-inductance of the stator is a function of the air gap, which is independent from the rotor angular position, since the rotor is non-salient type. Since the reluctance of the air gap is linear to the air gap length g, neglecting the magnetic resistance in the core, the self-inductance of stator windings, L may be approximated

$$L = \frac{M}{g_0 + z} + L_l \tag{1}$$

where, M is the effective inductance per unit air gap, g_0 is the nominal air gap length, z is the axial displacement of the rotor, and L_l is the leakage inductance. Since the stator phase are placed at 90° apart, mutual-inductance of the stator $L_{\alpha\beta}$ is zero. The self-inductance of the rotor winding L_f is written as

$$L_f = \frac{M_f}{g_0 + z} + L_{fl} \tag{2}$$

where, M_f is the effective inductance per unit air gap and L_{fl} is the leakage inductance. To simplify the analysis, letting $M = M_f$, the mutual-inductance between stator windings and the rotor winding $L_{\alpha f}$ and $L_{\beta f}$ change the angular position of the rotor as

$$L_{\alpha f} = \frac{M}{g_0 + z} \cos\phi \tag{3}$$

$$L_{\beta f} = \frac{M}{g_0 + z} \sin\phi \tag{4}$$

The circuit equation of stator windings are

$$v_\alpha = Ri_\alpha + p(Li_\alpha) + p(L_{\alpha f} i_f) \tag{5}$$

$$v_\beta = Ri_\beta + p(Li_\beta) + p(L_{\beta f} i_f) \tag{6}$$

where v_α and v_β are the terminal voltage of the stator windings, i_α and i_β are the current through the stator windings, i_f is the current through the rotor

windings, R is the resistance of the stator windings, and p is differential operator. Expanding equations (5) and (6), and transporting them, we have

$$\dot{i}_\alpha = \frac{1}{L}\left(v_\alpha - Ri - \dot{L}i_\alpha - \dot{L}_{\alpha f} i_f\right) \quad (7)$$

$$\dot{i}_\beta = \frac{1}{L}\left(v_\beta - Ri - \dot{L}i_\beta - \dot{L}_{\beta f} i_f\right) \quad (8)$$

The v_α and v_β in equations (7) and (8) switches very rapidly between V_s and $-V_s$ when the PWM amplifier is used. The $\dot{L}i$ can be neglected because it is small compared to $v - Ri$. Then assuming the leakage inductance is small, equations (7) and (8) are rewritten as

$$\dot{i}_\alpha = \frac{g_0 + z}{M}(v_\alpha - Ri_\alpha) \quad (9)$$

$$\dot{i}_\beta = \frac{g_0 + z}{M}(v_\beta - Ri_\beta) \quad (10)$$

These equations show a current waveform with high frequency ripple whose amplitude is proportional to the gap length between the rotor and the stator. Therefore amplitude demodulation will extract a signal which includes an air gap length information.

In the axial gap self-bearing motor, the driving voltage e_α and e_β are

$$e_\alpha = A\cos(\omega t) \quad (11)$$

$$e_\beta = A\sin(\omega t) \quad (12)$$

where, A is the amplitude of the alternating voltage, and ω is the angular velocity and t is time. These voltages are modulated to the pulse width form using the following a sawtooth wave.

$$e_c = \frac{2V_s}{\tau}t, \qquad -\frac{\tau}{2} \le t < \frac{\tau}{2} \quad (13)$$

where, τ is switching interval. Then terminal voltages become

$$v_\alpha = \begin{cases} V_s & -\frac{\tau}{2} \le t < \frac{A}{V_s}\cos(\phi)\frac{\tau}{2} \\ -V_s & \frac{A}{V_s}\cos(\phi)\frac{\tau}{2} \le t < \frac{\tau}{2} \end{cases} \quad (14)$$

$$v_\beta = \begin{cases} V_s & -\frac{\tau}{2} \le t < \frac{A}{V_s}\sin(\phi)\frac{\tau}{2} \\ -V_s & \frac{A}{V_s}\sin(\phi)\frac{\tau}{2} \le t < \frac{\tau}{2} \end{cases} \quad (15)$$

According to reference [7], the self-sensing output of each phase are calculated as

$$u_\alpha = \frac{V_s\tau}{4L}\left\{1 - \frac{A^2}{V_s^2}\cos^2(\omega t)\right\} \quad (16)$$

$$u_\beta = \frac{V_s\tau}{4L}\left\{1 - \frac{A^2}{V_s^2}\sin^2(\omega t)\right\} \quad (17)$$

These equations show that the self-sensing output is affected by the rotor angular position ωt, then it can not obtain the position signal. However, since the output of the each phase is a square of sinusoidal wave, the summation of each phase outputs becomes constant.

$$u_{\alpha+\beta} = \frac{V_s\tau}{4L}\left(2 - \frac{A^2}{V_s^2}\right) \quad (18)$$

TABLE 1: Simulation Parameters

Resistance R	2.2 [Ω]
Effective inductance M	4.0×10^{-6} [Hm]
Leakage inductance L_l	2.4×10^{-3} [H]
Nominal Air gap g_0	1.06×10^{-3} [m]
Equivalent Rotor Current i_f	0 [A]
Frequency of carrier	5[kHz]
Voltage of power source V_s	15[V]
Cut-off freq. of H. P. F.	1[kHz]
Order of H. P. F.	4
Cut-off freq. of L. P. F.	1[kHz]
Order of L. P. F.	4

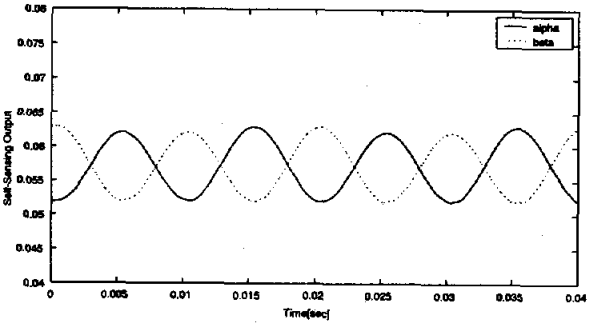

FIGURE 6: Self-Sensing Outputs ($A/V_s = 0.4, \omega =$ 50Hz, z=0mm)

Hence, it is possible to obtain the self-sensing output without the angular position of the rotor. However the self-sensing output is affected by the amplitude of the driving voltage and source voltage. Realization of the self-sensing control requires an air gap information without other influences. In order to obtain the output expressed with the function of only displacement, it is necessary to fix amplitude of the driving voltage or to compensate an output with a certain method.

SIMULATIONS

In order to confirm the previous analysis, self-sensing system is simulated using MATLAB/SIMULINK. Parameters of the model are shown in Table 1. These parameters are determined according to the experimental setup described later.

Figures 6 and 7 show the self-sensing output calculated from the each phase current waveform when $A/V_s = 0.4$, $z = 0$ mm. Figure 6 shows the results when $\omega = 50$ Hz, while figure 7 shows the resutls when $\omega = 100$ Hz. In both cases, the self-sensing output of phase α and β includes fluctuation of 180° phase different, and they have similar waveform to equations (16) and (17). Figure 8 shows the sum-

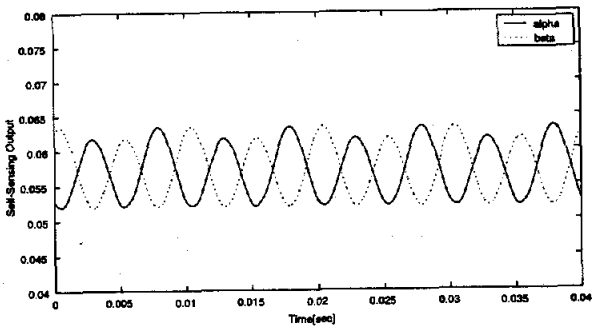

FIGURE 7: Self-Sensing Outputs ($A/V_s = 0.4, \omega =$ 100Hz, z=0mm)

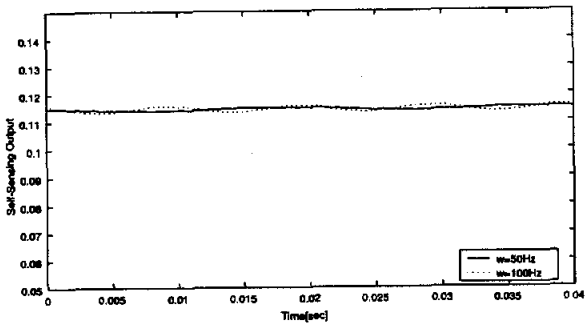

FIGURE 8: Averaged Outputs

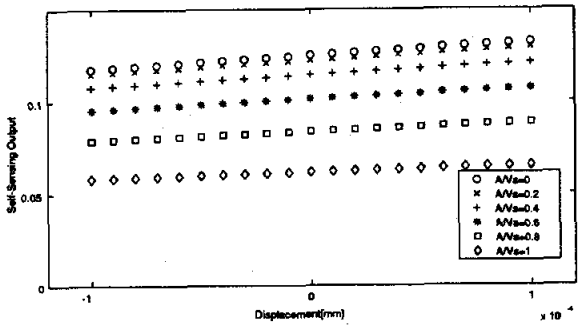

FIGURE 9: Self-Sensing Property

mation of self-sensing outputs of phase α and β. Although the resultant outputs have small fluctuation, almost constant outputs are obtained.

Figure 9 shows the output property for the air gap length at various amplitude of the driving voltage. When the amplitude of the operating voltage is fixed, the self-sensing output is linear the air gap length. However the self-sensing output changes considerably according to the voltage amplitude.

EXPERIMENTAL RESULTS

An experimental setup is made and tested as shown in figure 10. To confirm the static characteristics of the self-sensing output, the rotor is fixed on the

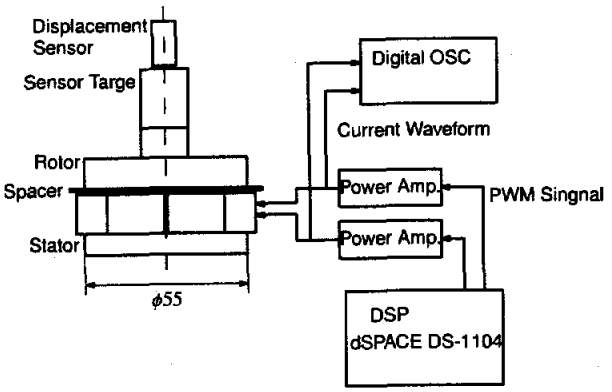

FIGURE 10: Experimental Setup

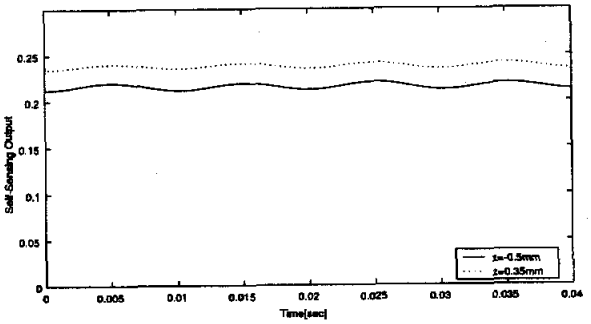

FIGURE 11: Self-Sensing Outputs

stator, and the spacer is inserted between the stator and the rotor. The displacement sensor is installed to measure the exact air gap length. The rotor disc and the stator have a diameter of 55mm and are made of the solid magnetic material. The stator has 8 concentrated wound poles each with 80 coil turns, and coils are connected to produce 4 pole, 2-phase flux.

In the digital signal processor, driving voltages are modulated to PWM signals, then the DSP outputs PWM signals to the power amplifiers. In the power amplifiers, the output voltage is switched between +15 V and −15 V according to PWM signal. The self-sensing output is calculated by the external computer. A current waveform of each coil is recorded by the digital oscilloscope, then it is transmitted to the computer. The computer calculates the self-sensing outputs numerically.

Figure 11 shows self-sensing outputs when the $A/V_s = 0.4, f = 50$Hz, $z = -0.5$ and 0.35 mm. Thes results indicate relatively large fluctuation compared with the displacement information. This is considered due to the time lag of the power amplifier. The theory and simulation is developed by assuming the voltage change instantaneously, but the amplifier used in the experiment was not fast enough. Figure

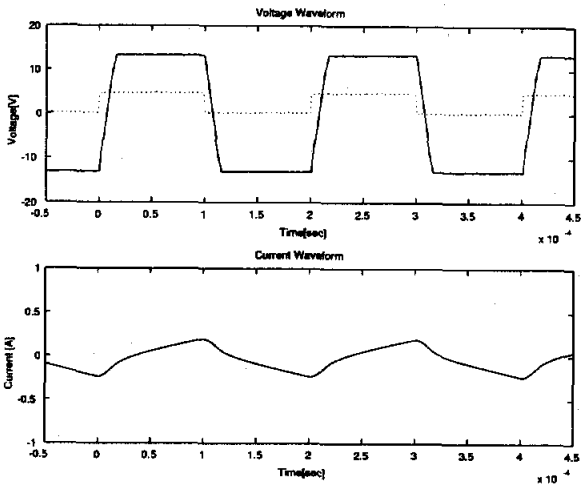

FIGURE 12: Switching Waveform

12 shows the switching waveforms. The upper graph shows the voltage waveform, while the lower graph shows the current waveform. The dotted line shows the PWM signal from the DSP. The switching takes 15 μsec. As a result, the current waveform has distortion as shown in figure 12, and the performance of the self-sensing output is deteriorated. It is expected that the performance of the self-sensing can be improved by improving the power amplifier. A newly designed switching power amplifier is planned to apply and the results will be reported near future.

CONCLUSIONS

This paper introduces a position self-sensing technique for an axial self-bearing motor. The air gap length is estimated by demodulating the switching frequency component of the PWM current waveform. The theoretical analysis shows that the self-sensing output of the each phase is the function of the driving vector, but the summation of the each phase self-sensing output becomes constant and independent from the angular position of the voltage vector. This is confirmed by the numerical simulation. However the experimental results are not good compared with the simulation. Future work is continuing to improve the self-sensing performance, and to realize of the self-sensing control.

References

[1] Okada, Y., Dejima, K., Ohishi, T., Analysis and Comparison of PM Synchronous Motor and Induction Motor Type Magnetic Bearings, IEEE Trans. on Industry Application, Vol. 32, No. 5, September/October 1995, pp. 1047–1053.

[2] Chiba, A., Deido, T., Fukao, T, Rahman, M. A., An Analysis of Bearingless Motor, Proc. of 5th Symp. on Magnetic Bearings, Kanazawa Japan, August, 1996, pp.313–318.

[3] Schöb, R., Bichsel, J., Vector Control of the Bearingless Motor, Proc. of Forth International Symp. on Magnetic Bearings, ETH Zürich, August 1994, pp. 327–332.

[4] Ueno, S., Okada, Y., Characteristics of Axial Force and Rotating Torque and Their Control of Permanent Magnet Type Axial Gap Self-Bearing Motor, Electrical Engineering in Japan, Vol. 132, No. 1, July 2000, pp. 81–91.

[5] Ueno, S., Okada, Y., Characteristics and Control of a Bidirectional Axial Gap Combined Motor-Bearing, IEEE/ASME Trans. on Mechatronics, Vol. 5, No. 3, September 2000, pp. 310–318.

[6] Mizuno, T. Bleuler, H., Gähler, C., Vischer, D., Towards practical applications of self-sensing magnetic bearings, Proc. of Third International Symposium on Magnetic Bearings, Tokyo, Japan, 1992.

[7] Noh, M. D., Maslen E. H., Self-Sensing Magnetic Bearing (Part I), Proc of Fifth International Symp. on Magnetic Bearings, Kanazawa, Japan, August 1996, pp. 95–100.

[8] Okada, Y., Matsuda K., Nagai, B., Sensorless Magnetic Levitation Control by Measuring PWM Carrier Frequency Component, Proc. of Third International Symp. on Magnetic Bearings, Alexander, USA, 1992.

[9] Matsuda, K., Okada, Y., Self-sensing Magnetic Bearing using Principle of Differential Transformer, Fifth International Symposium on Magnetic Bearings, Kanazawa, Japan.

[10] Matsuda, K., Okada, Y., Development of a Self-Sensing Control Technique for a Combined Motor-Bearing, 6th Motion and Vibration Control Symp., Chiba, Japan, March 1999. pp. 330–335 (in Japanese).